



UNIVERSITY OF LEEDS

This is a repository copy of *Improved Polymer Flooding in Harsh Environments by Free-Radical Polymerization and the Use of Nanomaterials*.

White Rose Research Online URL for this paper:  
<http://eprints.whiterose.ac.uk/143077/>

Version: Accepted Version

---

**Article:**

Haruna, MA, Nourafkan, E, Hu, Z et al. (1 more author) (2019) Improved Polymer Flooding in Harsh Environments by Free-Radical Polymerization and the Use of Nanomaterials. *Energy and Fuels*, 33 (2). pp. 1637-1648. ISSN 0887-0624

<https://doi.org/10.1021/acs.energyfuels.8b02763>

---

© 2019 American Chemical Society. This is an author produced version of a paper published in *Energy and Fuels*. Uploaded in accordance with the publisher's self-archiving policy.

**Reuse**

Items deposited in White Rose Research Online are protected by copyright, with all rights reserved unless indicated otherwise. They may be downloaded and/or printed for private study, or other acts as permitted by national copyright laws. The publisher or other rights holders may allow further reproduction and re-use of the full text version. This is indicated by the licence information on the White Rose Research Online record for the item.

**Takedown**

If you consider content in White Rose Research Online to be in breach of UK law, please notify us by emailing [eprints@whiterose.ac.uk](mailto:eprints@whiterose.ac.uk) including the URL of the record and the reason for the withdrawal request.



[eprints@whiterose.ac.uk](mailto:eprints@whiterose.ac.uk)  
<https://eprints.whiterose.ac.uk/>

# Improved Polymer Flooding in Harsh Environment by Free-Radical Polymerization and the Use of Nanomaterials

Maje Alhaji Haruna<sup>1</sup>, Ehsan Nourafkan<sup>1</sup>, Zhongliang Hu<sup>1</sup>, Dongsheng Wen<sup>1,2\*</sup>

<sup>1</sup> School of Chemical and Process Engineering, University of Leeds, Leeds, LS2 9JT, U.K.

<sup>2</sup> School of Aeronautic Science and Engineering, Beihang University, 100191, P.R.China

Email: [d.wen@leeds.ac.uk](mailto:d.wen@leeds.ac.uk), [d.wen@buaa.edu.cn](mailto:d.wen@buaa.edu.cn)

## Abstract

High temperature and high salinity (HTHS), and extreme pH conditions can significantly affect the stability of polymers and deteriorate the performance of polymer in enhancing oil recovery (EOR). This work advances polymer flooding in harsh environment on two fronts: engineering polymers with improved temperature tolerance, and dispersing suitable nanoparticles in the synthesised polymers to further improve their capabilities in withstanding temperature, salinity, and different pH conditions. Different modified acrylamide copolymers (polymer synthesized from two different monomers) and ter-polymers (polymer synthesized from three different monomers) are produced via free-radical polymerization and multi wall carbon nanotubes (MWCNTs) were introduced to obtain aqueous polymer dispersions with unique properties. The conversion, molecular weight and poly dispersity of co/ter-polymers were evaluated by <sup>1</sup>H-NMR, and GPC analysis. The interfacial, rheological behaviour and stability of the dispersions was investigated under HTHS conditions at various pH values to identify the suitable candidates for EOR applications. The oil recovery performance is examined in a core flooding set-up under 85°C and American Petroleum Institute (API) brine conditions. The polyampholytic ter-polymer and polyelectrolyte copolymer containing negative sulfonate

group showed improved viscosity and stability in the presence of MWCNTs in an alkaline and salinity conditions respectively. Comparing to pure polymer dispersions, the addition of MWCNTs to polymer improves oil recovery efficiency at high temperature (85 °C) in the presence of both alkaline pH and API brine conditions, yet with lower pressure drop. This, shows great promise for future EOR applications.

**Keywords:** Enhanced oil recovery; Polymer flooding; Multi wall carbon nanotubes; high temperature and high salinity; Rheology; Stability.

## 1. Introduction

After secondary (water-flooding) enhanced oil recovery (EOR), there are still considerable amount of residual oil remains trapped in reservoirs which can no longer be recovered using the conventional methods [1, 2]. Polymer flooding (PF) is one of the most successful chemical EOR processes in many depleted oil reservoirs [3]. Water soluble polymers have been investigated to enhance the viscosity of the displacing fluid, and improve the sweep efficiency, decreasing the oil-water mobility ratio [4].

Water-soluble polymers used in EOR are polyacrylamide (PAM) and its derivatives, with partially hydrolysed polyacrylamide (HPAM) being the most widely used [1, 5-9]. However, poor salinity resistance, low temperature tolerance, high susceptibility to oxidative degradation [10] and long flooding time [11] hinder the application of HPAM in most of the unconventional reservoirs. For instance Maghzi, A., et al [12] reported that HPAM would precipitate at high concentration of divalent cation ( $\text{Ca}^{2+}$ ,  $\text{Mg}^{2+}$ ) and undergo severe thermal degradation at high temperature. Therefore, in the last few decades attention has been given to improve the polymer performance in EOR. Salt tolerant and heat resistance polymers such as hydrophobically modified associating polymers [13], copolymers of acrylamide [14, 15], cationic polymers [16], thermoviscosifying polymers (polymers whose viscosity increases upon increasing temperature and salinity) [17] have been developed. Notwithstanding, there are still some shortcomings of those polymers that inhibit their applications in the field including adsorption, poor solubility, high cost and mechanical degradation [18]. Engineering new polymers that can withstand harsh environment is still a challenging task.

Very recently, the application of nanoparticles for EOR has emerged as an alternative technique to improve oil recovery efficiency. Both the properties of injected fluids (i.e., interfacial tension, viscosity, thermal conductivity) and the fluid-rock interaction properties (i.e., adsorption,

wettability alteration) can be engineered by using different nanoparticles [18-24]. Many of these studies have shown that inclusion of certain nanoparticles in a flooding fluid could increase the oil recovery rate [25-27]. Not surprisingly, these studies have been primarily focused on dispersing nanoparticles in a flooding fluid (i.e. brine), and the investigation of nanoparticle performance in a polymer solution is rarely conducted. The combination of nanoparticles and polymers could produce synergistic effects, leading to better oil recovery especially in harsh environment. Not directly related to enhanced oil recovery, there has been various investigations that have been conducted on the polymer-nanoparticle interactions. It has been seen that adding nanoparticles to polymers enhance their heat endurance capacity due to the strong interaction attributed to hydrogen bond formation between particle functionalities and amide groups of the polymers [6, 28]. The mechanical properties and reinforcement of polymer structures could be improved through nanoparticle interaction with carbonyl groups of the polymers, which serve as cross-linkers between the macromolecules [29-31]. Others have shown that the inclusion of certain nanoparticles could improve the thermal stability of polymers that can withstand harsh environment. Different nanoparticles such as silica [6, 12, 18, 32], layered double hydroxide [33-35], nano-clay [31, 36], and metal oxides [37], have been studied with a primary focus on improving polymer rheological properties.

This work aims to advance polymer flooding in harsh environment on two fronts: (i) engineering polymers with improved temperature tolerance, and (ii) dispersing suitable nanoparticles in the synthesized polymers to improve further their capabilities in withstanding high temperature, saline and alkaline conditions. Free-radical polymerization will be used to synthesize different co/ter-polymers based acrylamide skeleton, and multi-walled carbon nanotubes (MWCNTs) will be used to obtain aqueous polymer dispersions with improved properties. The elemental, morphological, interfacial, and rheological properties, plus the stability of engineered materials will be investigated under high temperature and high salinity

conditions, and a pilot study is conducted to explore their potential applications in enhanced oil recovery. MWCNTs are chosen in this work as they have strong interaction with the polymers [38-40]. The work advances state-of-art studies in two main aspects: development of new polymers, and new nanoparticle-polymer dispersions with improved properties, and performing a pilot study of these new materials for oil recovery in harsh conditions.

## **2. Material and methods**

### **2.1.Reagents and equipment**

Monomer of acrylamide (AA), isopropyl acrylamide (IAA), (3-acrylamidopropyl) trimethylammonium chloride (ATAC), 2-acrylamido-2-methyl-1-propanesulfonic acid (APSA), 4-4'-azo-bis-4-cyanopentanoic acid (ACPA), MWCNTs, calcium chloride, magnesium chloride, and sodium chloride were obtained from Sigma-Aldrich. Mineral oil with viscosity of 42 mPa s and density of 0.82 kg/m<sup>3</sup> were purchased from Kerax Ltd. (UK).

Proton NMR (<sup>1</sup>H-NMR) was used to evaluate the modification of co/ter-polymers using Advanced 500 Bruker Nuclear magnetic resonance (NMR) (resonance frequency of 400 MHz). Gel permeation chromatography (GPC) was also used to analyse the polymers to obtain the molecular weight and polydispersity using 0.1 M NaNO<sub>3</sub> as the mobile phase. The Agilent Technologies Infinity 1260 MDS instrument was used for the analysis, which was equipped with light scattering (LS), differential refractive index (DRI), UV detectors and viscometry (VS). Tosoh TSKGel GPWXL columns were set and operated at 40 °C with a 1 mL/min flow rate. The calibration was conducted between 106-1,368,000 g/mol using Poly(ethyleneoxide) standards (Agilent Easy Vials). The analysed samples were filtered before injection through 0.22 µm pore size hydrophilic GVWP membrane. Agilent GPC/SEC software was used to determine the experimental molar mass and dispersity values of synthesized polymers.

The nature of surface functionality species of the synthesised co/ter-polymers and their composites with MWCNTs was examined using ATR-Fourier-transform infrared spectroscopy (Nicolet iS10 FT-IR spectrometer). The morphology of the polymer/MWCNTs dispersion was investigated using transmission electron microscope (FEI Tecnai TF20 TEM). The stability of MWCNTs was performed to observe the flocculation and sedimentation during centrifugation of MWCNTs/polymer dispersion using a dispersion analyser centrifuge (LUMiSizer, Lum GmbH, Germany) by recording the transmission of near-infrared light. Viscosity ( $\eta$ ) of MWCNTs/polymers solution was measured using a Physica Anton Paar rheometer (Cone plate CP75-1, model MCR 301) at a shear range of 10-1000  $s^{-1}$  at 22 °C. Different frequencies ranging between 1 and 100 rad/s (i.e., 0.159 to 15.92 Hz) were used for dynamic frequency sweep measurement. Interfacial tension (IFT) and contact angle (CA) measurements were performed using a pendant drop tensiometer, equipped with a temperature controller and digital camera used for capturing the image of the droplet.

## **2.2. Polymer synthesis**

The polymers were synthesized from AA, IAA, APSA, and ATAC monomers based on the mass percentage describe in **Table 1**. The measured concentrations were individually dissolved in 180 ml deionized water in a round-bottomed flask. The flask was stirred in a water bath at 80 °C for 6 hours under reflux in the presence nitrogen gas following the addition of 10 mg ACPA as initiator to obtain free radical polymerizations.

To obtain polymer nanoparticle dispersions, the desired concentration of the MWCNTs were dispersed in brine (2 wt. %  $MgCl_2$ , 2 wt. %  $CaCl_2$  and 8 wt. %  $NaCl$ ), or in solution with different pH (acidic pH=3 or alkali pH=11). The mixture was sonicated using probe sonicator (Fisher scientific ultrasound probe) at an amplitude speed of 25 percent for 5 minutes to avoid particle aggregation. The synthesized polymer was then added into the suspension to obtain

MWCNTs/polymer dispersion and mixed by gentle stirring using a SB 162-3, Stuart magnetic stirrer for 24 h to allow sufficient time for the MWCNTs to associate with the graft polymer. A pH of the solution was regulated to acidic and alkali condition with hydrochloric acid and sodium hydroxide, respectively using pH meter (Seven Compact Mettler Toledo, UK). The brine solution was stored at a fixed temperature of 80 °C in an oven, and the stability test of immovable samples was conducted after 7 days.

**Table 1.** Different mixture of AA monomers during polymerization process.

<b>Properties</b>	<b>Sample A</b>	<b>Sample B</b>	<b>Sample C</b>	<b>Sample D</b>	<b>Sample E</b>
<b>AA (g)</b>	7.5	3.75	3.75	3.75	3.75
<b>IAA (g)</b>	0	0	0	0	1.875
<b>APSA (g)</b>	0	3.75	0	1.875	1.875
<b>ATAC (g)</b>	0	0	3.75	1.875	0
<b>Conversion %</b>	100	85	83	81	81
<b>PDI</b>	1.68	2.03	2.14	4.59	5.11
<b>M<sub>w, GPC</sub> (g/mol)</b>	499573	696575	636557	721406	1106656
<b>M<sub>n, GPC</sub> (g/mol)</b>	295696	343140	297457	157055	157055
<b>Substitution ratio (%)</b>	AA:100	APSA:51.6- AA:48.4	ATAC:53.9- AA:46.1	APSA:32.9- ATAC:28.7- AA:38.4	APSA:25.3- IAA:30.5- AA:44.1

### **2.3.Preparation of Porous medium and Core-flooding setup.**

For preparation of core flooding, the Ottawa sands were packed into a metallic column by conducting a sequence of rigorous procedures for wet-packing to determine relatively constant porosity and permeability values for various packing based on the procedure obtained from [27]. The resulting parameters obtained for the column are recorded in **Table 2**.

To evaluate the EOR potential for polymer and polymer/MWCNTs dispersions, a core-flooding set up was prepared as illustrated in **Fig. 1**. During the flooding process, a piston pump

(series I, Core-Palmer Instrument Co. Ltd) was used for brine injection. A syringe pump (KDS 410, KD Scientific Inc. USA) was employed for mineral oil injection and a new syringe was used for the injection of each sample to avoid cross contamination of the samples. A pressure transducer (150 psi, Omega Engineering Ltd.) was applied for measuring the pressure drop while carrying out the experiments. The heating was supplied and controlled by the EZ-ZONE PM Integrated PID Model. There are three K-type thermocouples (5TC-TT-K-36-36, a diameter of 0.13 mm and a precision of  $\pm 0.5$  K, Omega) attached to the both ends and the middle of the stainless steel core holder. They are parallel twisted together and feed the average temperature back to the controller as a process signal. The target temperature of the controller was set at 85 °C, and the output power of heating tape (SRT051-040, OMEGA) was controlled by a PID control loop based on the difference between the set temperature and the process temperature from those three parallel-twisted thermocouples. The following procedure was used for the core flooding investigation:

- The core was saturated with the brine by injecting at least 100 mL of API brine (2 wt. %  $\text{CaCl}_2$  and 8 wt. % NaCl) into the packed column at a continuous flow rate of 2ml/min. This resulted in a thoroughly saturated column thereby allowing sufficient time for sand grain deposition.
- The column was saturated with the oil by injecting 20 mL of high viscous mineral oil at constant flow rate of 0.5 mL/min until achieving water saturation of  $S_{wi} = 25\%$ .
- Secondary oil recovery stage using brine flooding was executed by injecting 3 pore volume (PV) at a constant flow rate of 0.5 mL/min.
- Tertiary flowing was performed at a similar flow rate of 0.5 mL/min using polymer or polymer/MWCNTs samples.
- The effluent liquid was collected in 50 ml graduated cylinder marked in 0.1 mL division in order to know the actual oil recovery.

- The overall oil recovery, and the tertiary recovery factors were calculated by polymer or MWCNT/polymer dispersion flooding.
- The temperature was maintained at 85 °C during the whole process.

**Table 2.** Average value of parameters for packed sands column.

Porous media properties	Values	Uncertainties (%)
Bulk volume (mL)	33.7	4.7
Pore volume (mL)	12.8	5.4
Porosity (%)	38.23	6.5
Absolute permeability (mD)	95	6.8
Mass of dry sands (g)	53.5	6.7
Liquid in the pore space (g)	12.8	3.9
Temperature (°C)	85	1.7

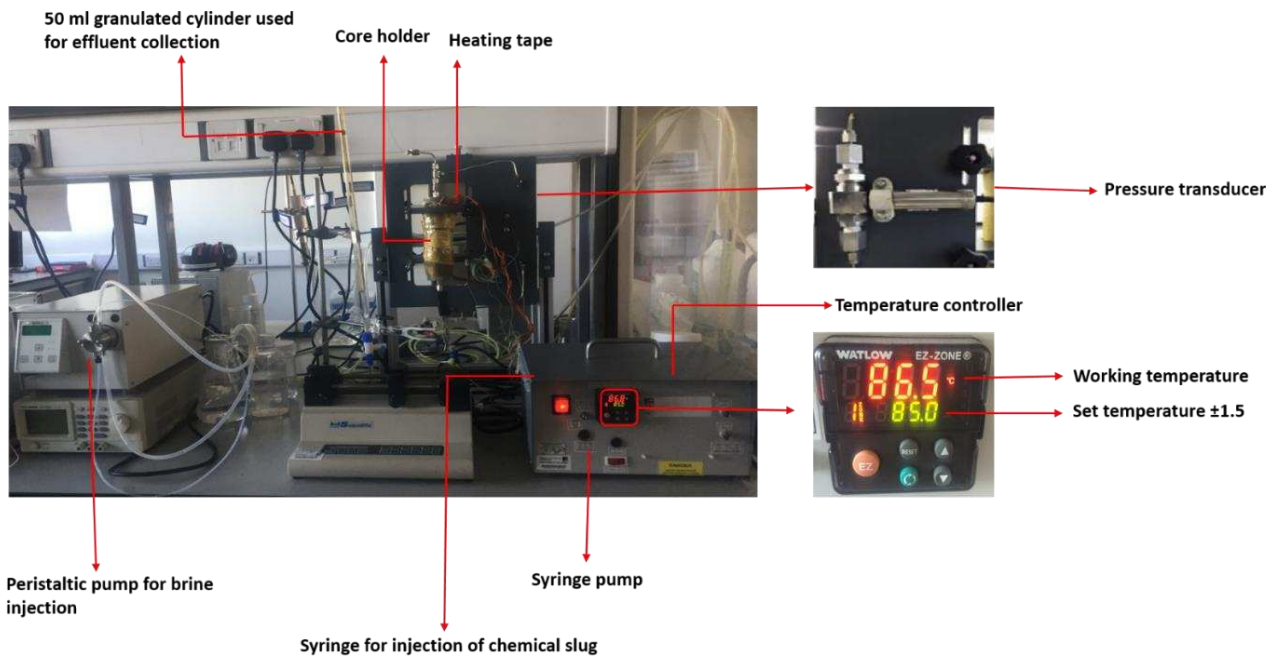


**Figure 1.** Experimental setup for core flooding

### 3. Results and discussion

#### 3.1. Characterization of Co/ter-polymer and MWCNTs/polymer hybrid

The structure of the synthesized polymers consisted of hydrophilic molecular chains with different neutral random side chains viz: hydrophobic, cationic or anionic as shown in **Fig. 2**. <sup>1</sup>H-NMR spectra of the co/ter-polymers were recorded after dissolving 10000 ppm in a 1:10 deuterium oxide (D<sub>2</sub>O) to and water solution at 25 °C. The analysed NMR spectra of the synthesized polymers are shown in **Fig. S1** supporting documents. The conversion of polymers was obtained by calculating the NMR resonance ratio between the monomers and polymer units, as proposed by the equation below [41].

$$Conversion = \frac{S_p}{S_p + S_m} \dots \dots \dots Eqn. (1)$$

Where S<sub>m</sub> stands for the peak area of the monomer and S<sub>p</sub> represent the peak area of the obtained polymer. The conversions at the end of co/ter-polymerization have been reported in **Table 1**. The MastReNova software, (Mestrelab research S.L., version 6.0.2) was used to measure the integration peaks that contributed to the functional groups. For instance, in the <sup>1</sup>H-NMR spectra of sample B, the integration peaks that appear for the functional groups of APSA and AA monomers after they react are 3.41 and 3.2 (equivalent to 51.6 and 48.4 substitution percent), respectively as illustrated in **Fig S1i**. The substitution percent of the remaining samples are shown in **Table 1**.

The polydispersity index (PDI), the weight average molecular weight (M<sub>w</sub>), and number average molecular weight (M<sub>n</sub>) of the polymers obtained by GPC are compiled in **Table 1**. The outcome show that the polydispersity of polymers increased when different monomers were used during polymerization. The minimum and maximum PDI belong to pure acryl amide polymer and partially hydrophobic polymers respectively. The higher M<sub>w</sub> and PDI of partially hydrophobic polymers shows the high molecular weight in sample E has a significant influence

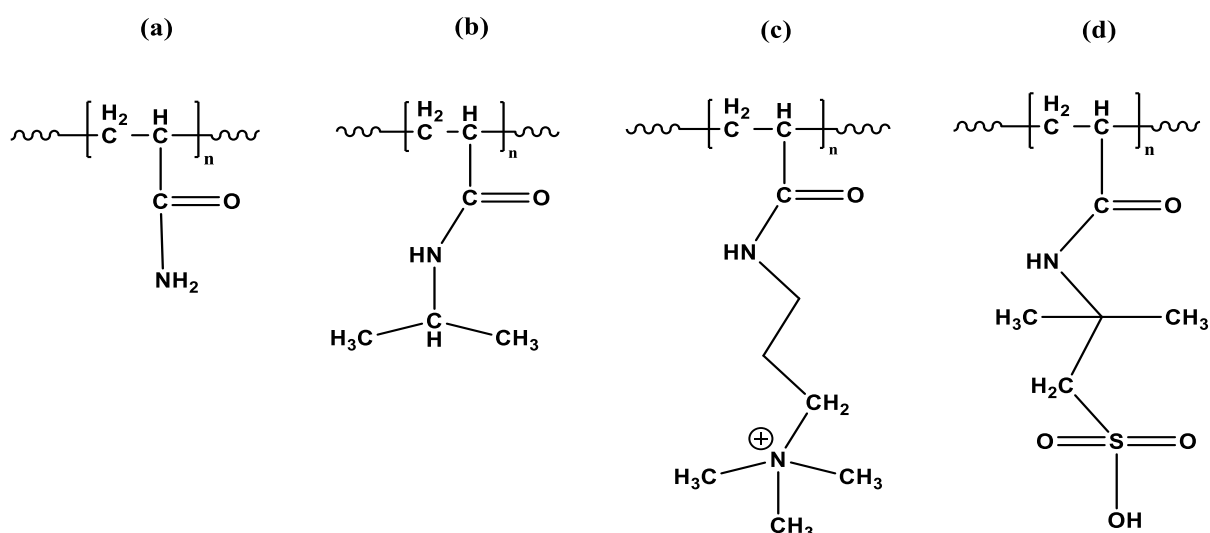


**Figure 2.** Schematic of side chains in co/tar-polymers molecular structure (a) Amide side chain, (b) Hydrophobic side chain (c) Cationic side chain and (d) Anionic side chain.

**Fig. 3** depicts the ATR-FTIR spectra of different co/ter-polymers and the dispersions of polymer/MWCNT. In the polymer spectra, it was observed that the adsorption peak of APSA anionic polymer containing  $\text{SO}_3$  group appeared at  $1040 \text{ cm}^{-1}$  [42, 43]. The absorption band observed at  $1037 \text{ cm}^{-1}$  for copolymers containing APSA (sample B and D) decisively shows the presence of anionic monomers in the structure of the copolymer, which confirms the existence of the  $\text{SO}_3$  group stretching vibrations. The vibrations observed at  $967 \text{ cm}^{-1}$  in sample C and D are attributed to the quaternary ammonium group in the ethoxylated group of ATAC cationic polymer [44, 45]. The adsorption bands at  $1649 \text{ cm}^{-1}$  and  $2930 \text{ cm}^{-1}$  were derived from C=O bonds and C-H stretching vibration, respectively. On the other hand, the ATR-FTIR spectrum of polymer/MWCNT composites shows almost all the peaks that appear in the net polymer samples but most of the peaks become weaker. Because in ATR-FTIR, the detection depth is normally between 1 to  $2 \mu\text{m}$ , but it can vary depending on the materials, for instance, black sample (e.g. MWCNTs/polymer) is a highly absorbing material which tends to have smaller sampling depths causing the signals to be weak. New peaks at around  $2200 \text{ cm}^{-1}$  are

attributed to the CN stretching vibration emerging from the  $\text{NH}_2$  group in PAM and CO in the nanocomposites.

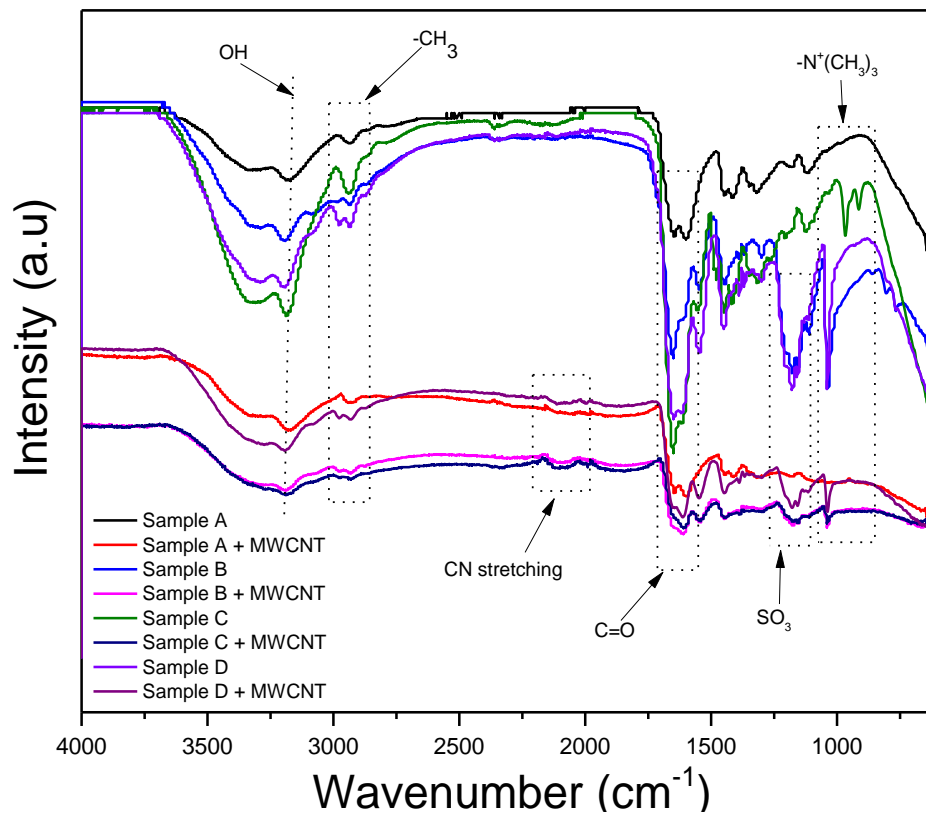


**Figure 3.** FTIR analysis of co/ter-polymers and polymer/MWCNT composites.

### 3.2. Stability analysis

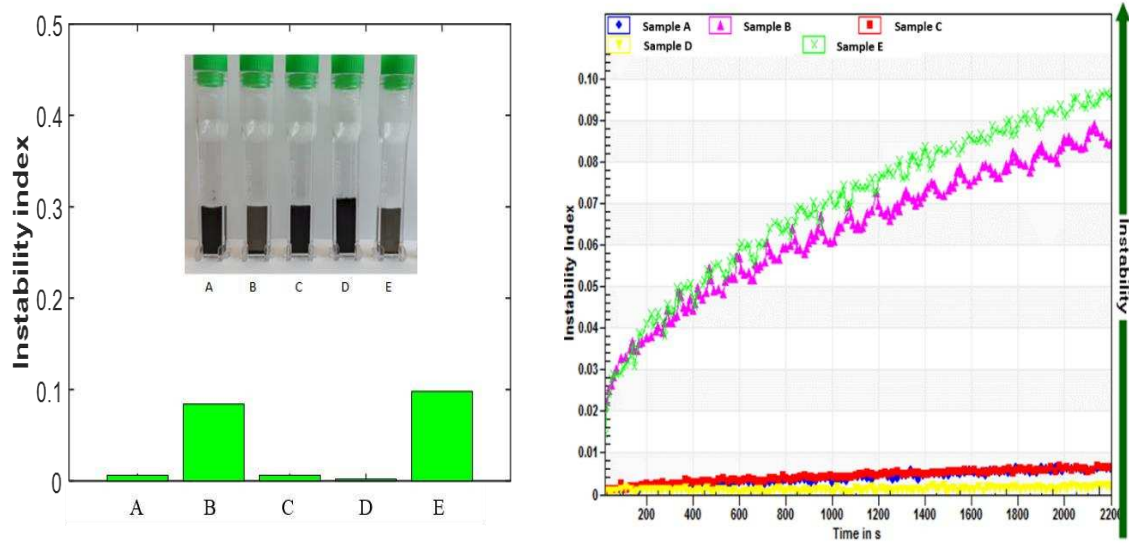
Polymer/MWCNTs adsorption and stability were investigated using experimental [46-48] and MD simulation methods [40, 49]. As reported, two main factors that influence the stability of the MWCNTs in solution are the electrostatic repulsion between polymer chains when counterions exist and the interaction of the polymer side chains with the aqueous phase. It has been reported that, flocculation of MWCNTs in the composites under severe conditions causes phase separation in an aqueous medium. The most common cations present in oil reservoirs are  $\text{Na}^+$ ,  $\text{Ca}^{2+}$  and  $\text{Mg}^{2+}$ , which interact with the polyelectrolytes and deteriorate the polymer performance [50]. In this work, an analytical centrifugation dispersion analyser (LUMiSizer

6110) has been used to investigate the stability of the formed MWCNTs/polymer nanocomposites under harsh conditions.

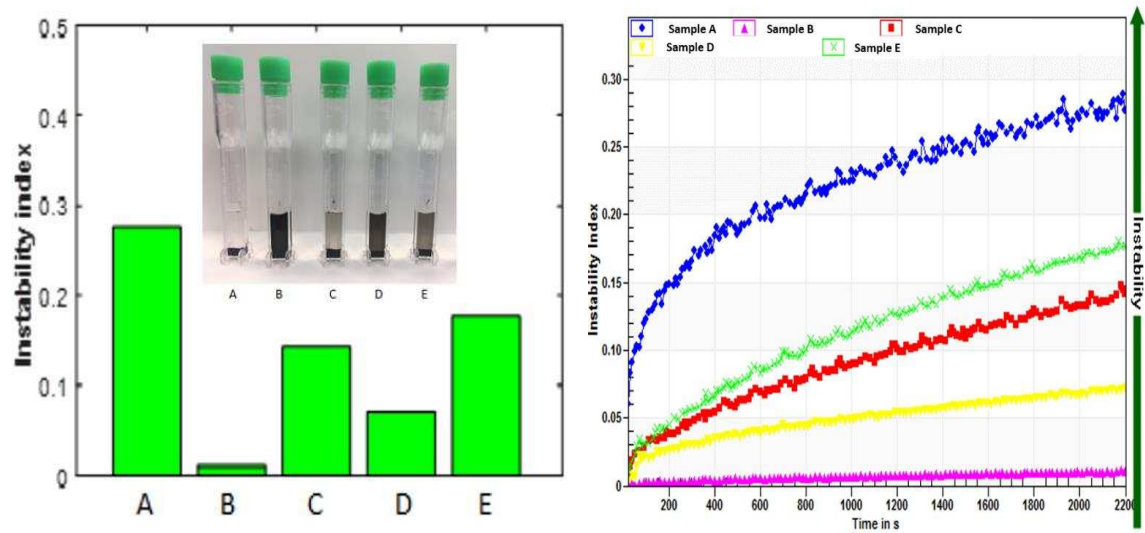
Polycarbonate capillary cells were filled with 0.5 ml of MWCNTs/polymer dispersion and centrifuged at 3000 rpm for 36 min which correspond to 1 month in actual conditions. **Fig. 4** shows the dispersed MWCNTs containing negative sulfonate-functional group shows lower stability at acidic pH. This is presumably because of the effect of positive molecular proton ( $H^+$ ) on the sulfonate groups. In contrast, the deprotonation of sulfonate groups on the copolymer was higher at alkaline pH rather than acidic pH which contributes substantially to electrostatic repulsive force between functionalized MWCNTs. Comparatively, high stability of dispersed MWCNTs/sample C was observed in positive groups of copolymer containing quarterly ammonium side chains at acidic pH, because the polymers were protonated more effectively in low pH conditions. The effect pH variation has less significance on the stability of MWCNTs in solution. However, MWCNTs were shown to be unstable at both acidic and alkali pH in the presence of positive-negative side chains in the polyampholytic polymer structure (sample D) as shown in Fig. 4 (c). Furthermore, copolymers consisting of negative sulfonate functional groups (sample B) demonstrated outstanding stability in high temperature-high salinity conditions. This is because the copolymer containing sulfonate groups can withstand divalent ions and sustain the steric repulsive forces between polymer branches and the solubility of skeleton acrylamide at high salt contents [51-53]. Therefore, the negative sulfonate group prevented the collapse of the polymer backbone by attracting both mono and divalent ions inside API brine thereby protecting the chains repulsion of the acryl amide chains as presented in Fig. 4 (b). Fig. 5 shows the TEM images of the MWCNTs and sample B/MWCNTs as an example to illustrate the stable dispersion and microstructure of polymer/MWCNTs solution. MWCNTs show an array of concentric cylinders, polymer/MWCNTs displayed an excellent dispersion ability, showing polymer has been

grafted to the MWCNTs, which could be used to confirm the appearance of chemical bonds between the polymer and MWCNTs. Moreover, the way the MWCNTs superimpose with polymer is an evidence that the polymer-MWCNTs interaction is a strong chemical adhesion and not a mere physical contact.

(a)



(b)



(c)

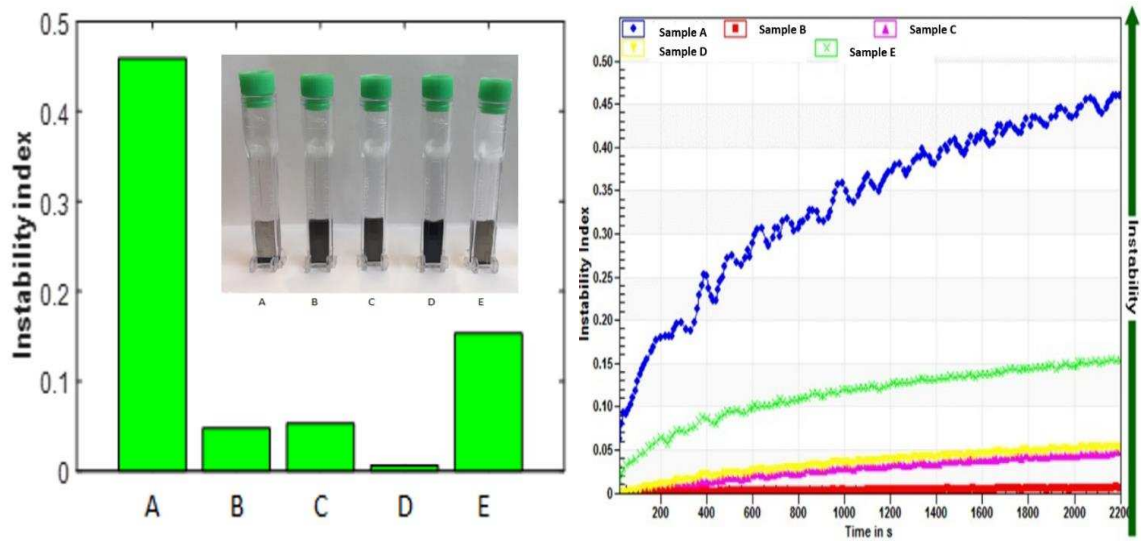


**Figure 4.** Instability index of MWCNTs (1000 ppm)/polymer (1000) at (a) normal condition, (b) API brine and (c) pH=11.

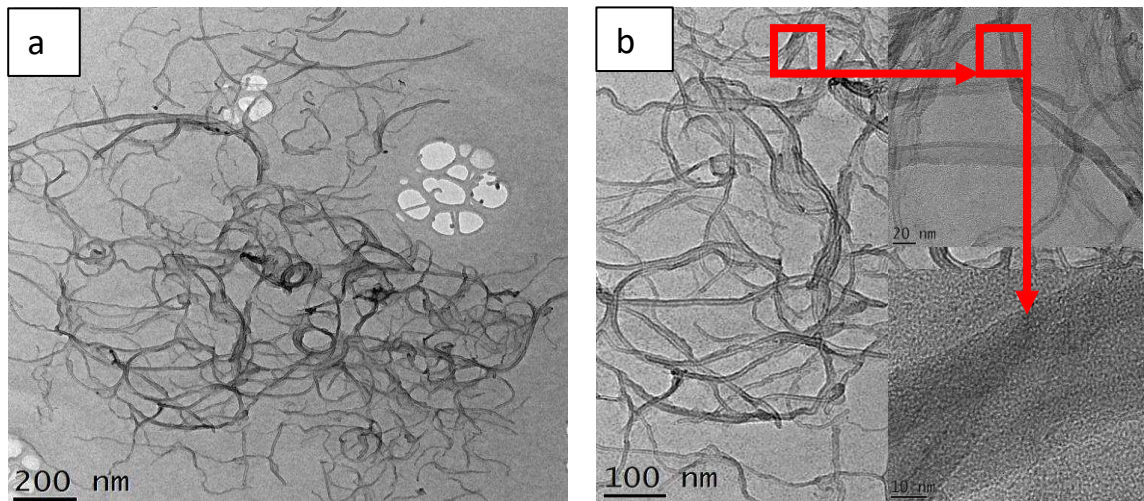


**Figure 5.** TEM photo of (a) MWCNTs and (b) MWCNTs/polymer (sample B) at different magnification.

### 3.3. Rheological investigation

Rheological investigation is a key factor in the polymer flooding process. In order to achieve an optimum oil recovery, an accurate viscosity of the polymer is required to obtain favourable mobility ratio between the oil and displacing fluid. However, the polymer viscosity is affected by the temperature and salinity present in the oil reservoirs [10, 50, 54, 55]. Both salinity and temperature cause different mechanisms on PAM viscosity reduction. Higher temperature results in the diminishing of the copolymer hydrophobic effect between the polymer chains and

speed up polymer solubility, and hence decreases its viscosity [50, 55]. Whereas, in the presence of salinity, the ionic shielding on the amide groups ( $\text{CONH}_2$ ) in the chemical structure of PAM reduces the chains' repulsion of the PAM backbone which results in the collapse of polymeric coils and reduction in polymer size and hence more viscosity reduction [10, 55].

However, the addition of nanoparticles into the polymer backbone enhances its rheological behaviour at high salinity and high temperature. As shown in **Fig. 6**, different approaches such as covalent linking, complexation through the interactions and wrapping of  $\text{NH}-\pi$ ,  $\text{CH}-\pi$ ,  $\pi-\pi$  were proposed using polymers and functionalized MWCNTs composites [47, 56-59]. These multi point interactions strengthen the polymer chains resulting in enhanced internal friction between the polymer chains and the molecules of the neighbouring solvents, thus improving the solution viscosity.

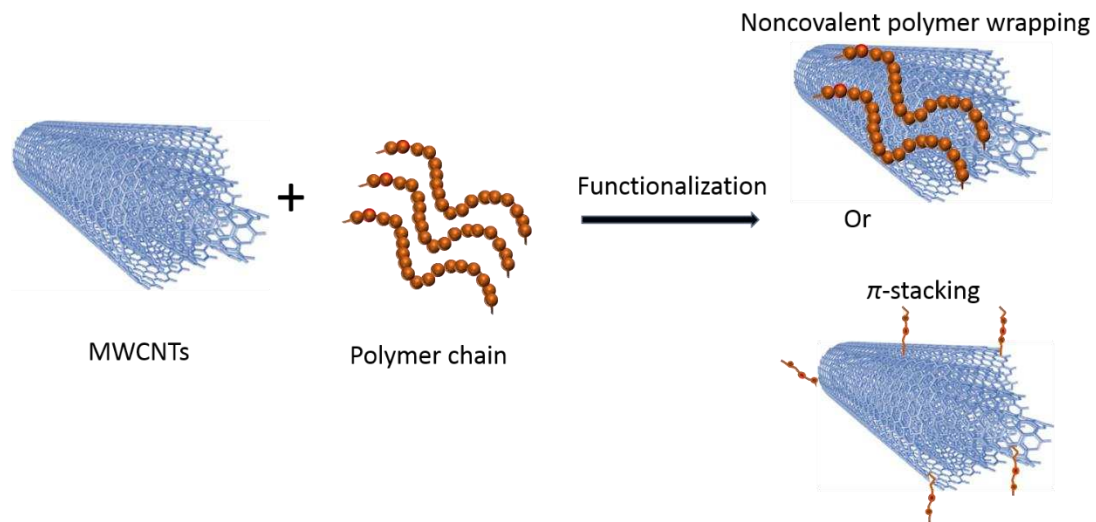


**Figure 6.** Schematic illustration for different sequence for MWCNTs functionalization via noncovalent polymer wrapping or  $\pi$ -stacking.

The current work investigates the viscosity of polymer/MWCNTs composites at high temperature in the presence of API brine and alkaline pH. **Fig. 7a** demonstrate the viscosity of 1000 ppm co/ter-polymers as a function of shear rate at 85 °C. The results indicated that after

the incorporation of hydrophobic chains in pure acrylamide structure (Sample A), the viscosity of the modified samples improved, and this enhancement of viscosity would be ascribed to the intermolecular hydrophobic association of polymeric chains. However, the hydrophobic chains combined to reduce self-exposure in the aqueous medium resulting in an increase of apparent viscosity, similar to what Hussein and co-workers [60] observed in which the addition of a hydrophobic fraction improved the polymer structure and increased the viscosity.

**Fig. 7b** demonstrate the viscosity of polymer/MWCNTs at alkaline pH. A reduced value of viscosity for all polymers at pH = 11 with increasing shear rate was observed because of a high hydrolysis degree in the presence of OH<sup>-</sup> ions and these results are consistent with some early studies [54, 61, 62]. However, the decrease in viscosity was lower in sample B and D (polymer containing negative group) than the other samples. This is due to enhanced intermolecular interaction between the polymer containing negative groups and the MWCNTs in comparison to other functional groups due to the presence of sulphate group as confirmed by FTIR analysis. The interaction was found to be stronger, specifically at higher shear rate which produced greater internal friction. Several investigations [51, 63] also reported high temperature resistance by the polymer containing sulfate and sulfonates groups.

**Fig. 7c** highlights the influence of salinity on the viscosity of polymer/MWCNTs at 85 °C. Correspondingly, the polymer containing negative groups (sample B) showed better salinity resistance, while the cationic polymer (sample C) showed less salt tolerance. The reason is that the positive group in the polymer is compatible to monovalent and divalent ions (Na<sup>+</sup>, Mg<sup>2+</sup> and Ca<sup>2+</sup>), which results in mutual repulsion and shields the amide negative groups in the co/ter-polymer chemical structure and therefore causes a reduction in viscosity.

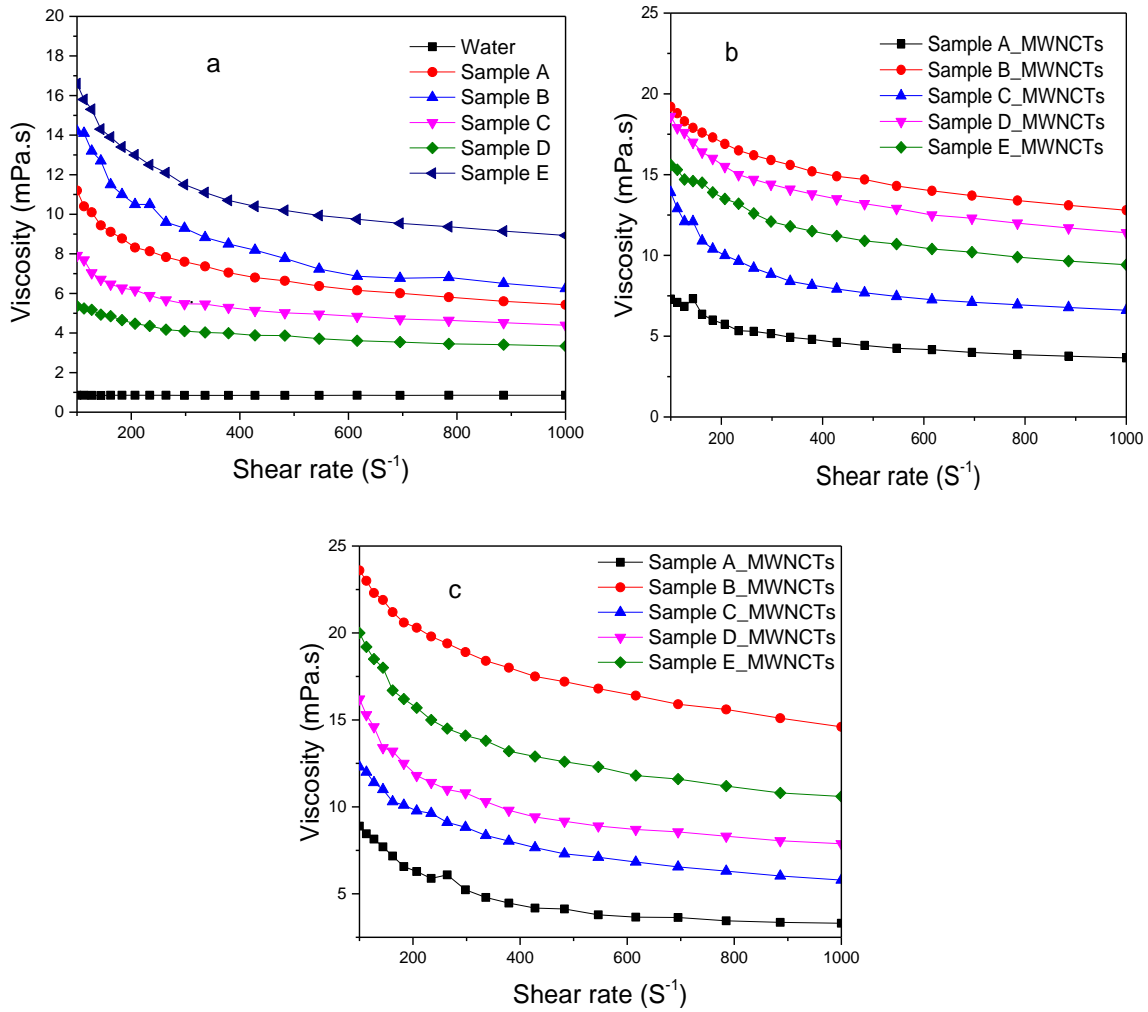


**Figure 7.** Dependent of viscosity on shear rate for (a) pure co/ter-polymers (1000 ppm) in water, (b) MWCNTs (1000ppm/1000ppm) in pH-11 and (c) polymers/MWCNTs (1000ppm/1000ppm) in API Brine, all measurement was conducted at 85 °C and shear rate 100-1000 S<sup>-1</sup>.

### 3.4. Selection of proper samples for EOR experiment

The best polymer for core flooding investigation was selected based on the stability and rheological analysis. **Table 3** and **Fig. 8** shows a brief summary for the evaluation of different polymer/MWCNTs dispersion samples. The study indicates that the polyelectrolyte copolymer and polyampholytic ter-polymer containing the negative sulfonate group (sample B and D)

improved the stability and viscosity in both saline and alkaline conditions, and are thus considered as better candidates for the core flooding experiment.

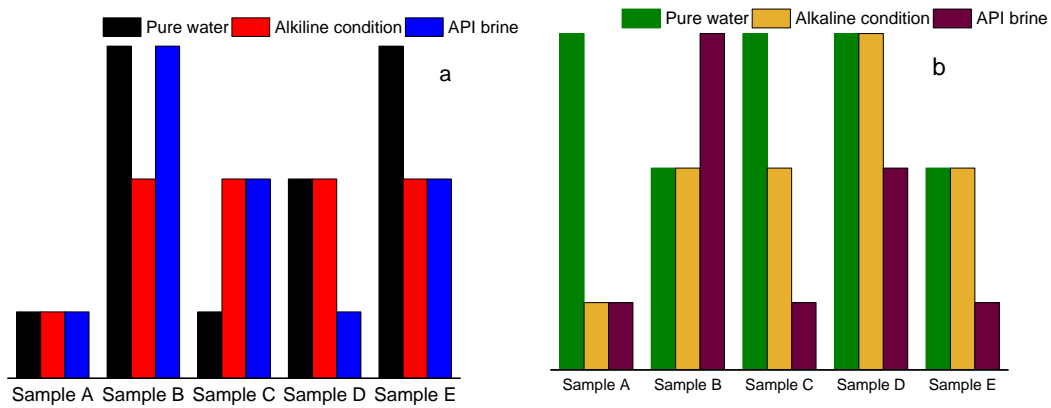


**Figure 8.** Summary of the (a) viscosity and (b) stability evaluation of different MWCNTs/polymers.

**Table 3.** Viscosity and stability evaluation of different MWCNTs/polymers.

Condition	Sample A		Sample B		Sample C		Sample D		Sample E	
	Viscosity (85 °C)	Stability (60 °C)								
Water	Weak	Good	Good	Fair	Weak	Good	Fair	Good	Good	Fair
Alkaline condition	Weak	Weak	Fair	Fair	Fair	Fair	Fair	Good	Fair	Fair
High salinity	Weak	Weak	Good	Good	Fair	Weak	Weak	Fair	Fair	Weak

Viscoelastic behaviour of the selected samples was investigated before the EOR experiment. Both storage ( $G'$ ) and loss ( $G''$ ) moduli increased after the addition of MWCNTs, as shown in **Fig. S2** in the supporting document. Four different reaction mechanisms are accountable for the changes in viscoelastic properties of the polymers [64], these are (a) MWCNTs/polymer network where the polymer shape could be entangled or adsorbed on the nanotube, (b) MWCNT-MWCNT network due to overlap of two nanotubes, (c) temporary entanglements of polymer network to form polymer matrix and (d) MWCNTs bridging by polymer. The

crossover of modulus (where  $G' > G''$ ) represent characteristic relaxation times, which is in agreement with the time for a MWCNTs to circulate a distance similar to its length [65]. At low MWCNTs concentration the relaxation could be identified across a section but it tended to increase with increasing concentrations because of the slowing of nanotube diffusion and ability of the solution to act in similarity to an elastic solid [65].

### 3.5. Oil recovery efficiency

A series of core flooding investigations (runs 1-6) were conducted for the two best selected polymers and their dispersion with MWCNTs, also bare co/ter-polymer was tested as a reference to examine MWCNTs effect on incremental oil recovery. The experimental conditions and the results of oil recovery efficiency with the uncertainty of 0.2% are summarized in **Table 4**. Also **Fig. 9a** shows the accumulated oil recovery efficiency by co/ter-polymer, copolymer containing negative sulfonate group (sample B) and its composites with MWCNTs at high temperature (85 °C) and high brine salinity (2 wt.%  $MgCl_2$ , 2 wt.%  $CaCl_2$  and 8 wt.%  $NaCl$ ), relative to the original oil in place (OOIP) after oil saturation for secondary and tertiary flooding, respectively. It can be seen that, the polymer/MWCNTs improved the oil recovery by 14.8% OOIP (from 70.2% to 85%) in the tertiary recovery stage while the copolymer containing negative sulfonate group and bare co/ter-polymer increase the recovery by 10.6% and 7.6% respectively. The photos of recovered oil for each case can be found in **Fig. S3** supporting documents.

On the other hand, **Fig. 9b** demonstrates the results of accumulated recovered oil after flooding with co/ter-polymer, copolymer containing positive-negative group (sample D) and its composites with MWCNTs at high temperature (85°C) and pH=11. Similar to the above findings, the composites of positive/MWCNTs show a higher oil recovery of 10.8 % (from 70.5% to 81.2%) whereas the copolymer containing a positive-negative group and bare co/ter-

polymer increase the recovery by 8.7% and 7.0% respectively. The photos of recovered oil for each case can be found in **Fig. S4** supporting document.

The greater recovery factor by the polymer containing MWCNTs in both experimental conditions revealed outstanding capability of the composites to modify oil/water mobility ratio. However, higher oil recovery could be attributed to the high viscosity of the composites compared to other tested samples, and its ability to perform under high temperature and high salinity without losing much of its viscosity. The polymer/MWCNTs displayed greater rigidity in the porous medium due to its reasonable viscous force when it flowed in the core plug, whereas bare polymers were believed to lose a considerable viscosity fraction in the porous medium, specifically at high temperature and high saline conditions. Thus, a larger area of the core could be swept by polymer/MWCNT solution without the fingering effect and hence more oil recovery was achieved. Although the copolymer containing negative sulfonate group has around 3% higher oil recovery compared to bare co/ter-polymer, this could be due to the greater salinity resistance exhibited by the modified sulfonate group as explained above. Generally, it can be deduced that polymer/MWCNTs flooding, could be more successful over the other samples because of its better mobility control, which has been achieved by enhancing the rheological properties of the solutions.

**Table 4:** Oil recovery efficiency by using polymer and polymer nanoparticles composites

Displacing Fluid	Efficiency after brine flooding, % OOIP	Efficiency after tertiary flooding, % OOIP	Enhance oil recovery efficiency, %
Sample A (API)	65.6	73.2	7.6
Sample B (API)	67.2	77.7	10.6
Sample B + MWCNTs (API)	70.2	85	14.8
Sample A (pH-11)	67.9	74.9	7.0
Sample D (pH-11)	68.9	77.6	8.7
Sample D + MWCNTs (pH-11)	70.5	81.2	10.8

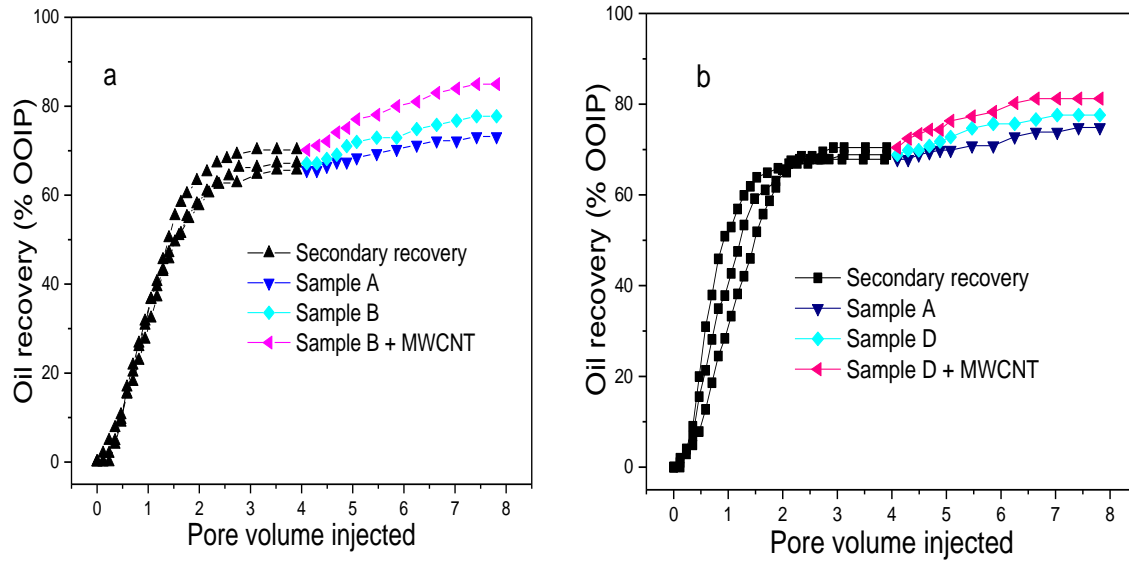


**Figure 9.** Tertiary oil recovery obtained by (a) co/ter-polymer (sample A), copolymer containing negative sulfonate group (sample B) and its composites (sample B + MWCNTs) at high temperature (85 °C) and high brine salinity (2 wt.% MgCl<sub>2</sub>, 2 wt.% CaCl<sub>2</sub> and 8 wt.% NaCl, ) and (b) co/ter-polymer (sample A), copolymer containing positive-negative group (sample D) and its composites (sample D + MWCNTs) at high temperature (85 °C) and pH =11.

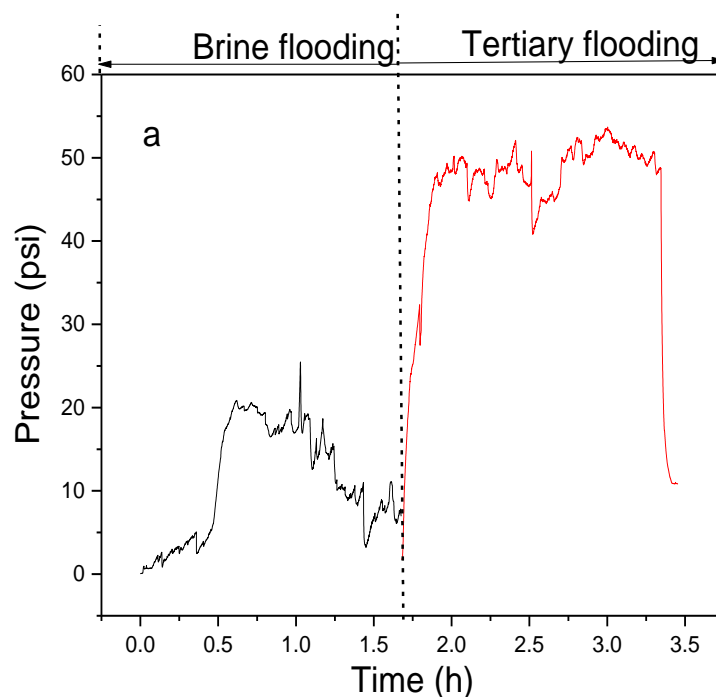
The results of the interfacial surface tension (IFT) and contact angle (CA) for all 6 samples are shown in **Table 5**. An alteration is observed for both factors with the addition of MWCNTs to the polymer solutions at high salinity and alkaline pH conditions. According to the results, the wettability was changed towards neutral-wet status with the addition of MWCNTs. The CA for pure polymer solutions was found to be between 40° to 42° in both high salinity and alkaline conditions. The results show that the addition of MWCNTs changes the CA slightly from 42° to around 36°. Similarly, the IFT values are also decreased slightly with the addition MWCNTs into the fluids. However, two different scenarios were observed for IFT reduction, at API brine condition the fluids IFT is 34 mN/m while 55 mN/m was observed at pH=11. This may be because of the salt capability to enhance the adsorption rate at the oil water interface which

account for the compression of the electrical double layer [66]. The weakening of the electrical double layer enhances the molecules transfer faster from bulk-phase to oil-water interface and thus reduces the value of IFT [66]. It was also mentioned that the addition of NaCl decreases the solubility rate of the injected fluid, and makes it more ionized, and thereby it adsorbs more strongly at the oil-water interface which reduces the IFT value [67]. With addition of MWCNTs, the IFT values for sample B reduced from 34 to 28 mN/m whereas that of sample D reduced from 55 to 47 mN/m respectively. This IFT reduction proves the nanoparticles capability to mobilize the oil, leading to easy flow of targeted oil by reducing the energy required by oil droplets to flow through the pore throat.

The differential pressure recorded during oil recovery analysis for the core flooding investigation for the copolymer containing negative sulfonate group (sample B) and sample B/MWCNTs at high temperature (85 °C) and high brine salinity (2 wt.% MgCl<sub>2</sub>, 2 wt.% CaCl<sub>2</sub> and 8 wt.% NaCl) are shown in **Fig. 10**. It can be observed in **Fig. 10a** that pressure drop increases after the injection of the bare polymer whereas, after injecting the solution of MWCNTs in copolymer containing negative sulfonate group we observed that the pressure drop became lower than that after brine injection (**Fig. 10b**). Contrary to the conventional thought that the MWCNT dispersion has higher viscosity than the pure polymers and would have greater possibility to form a wedge or block the pore channel, thereby causing the pressure drop to increase, the reverse was observed. This implies that MWCNTs play a leading role in enhancing the fluidity while moving along the pores, and also have the tendency to reduce the cost associated to polymer flooding as it lowers the amount of energy required during the injection process. Similar observation was made in the case of the copolymer containing positive-negative sulfonate group (sample D) and its composites (sample D + MWCNTs) at high temperature (85 °C) and pH=11 (the results are reported in **Fig. S5**

supporting documents). Nevertheless, the pressure drop for the MWCNTs/polymer sample is even lower than that of the brine injection.

Considering these results, it was assumed that polymer/MWCNTs dispersions altered the surface condition of the core sample to become more hydrophilic during the nanofluid injection [68, 69]. As explained, both copolymers containing negative and positive-negative groups are hydrophilic in nature with anionic and cationic side chains, but, the addition of MWCNTs makes them more hydrophobic, promoting partial interaction between the particles and demonstrate electrostatic repulsion against the pore surface. Such partial but lengthy hydrophobic attraction of the hybrid materials would advance the formation of a favourable wedge film, created by disjoining pressure, hence causing incursion of the nanofluid to the oil wet glass surface [69]. This wedge film easily changes the surface wettability of the oil drop against the glass surface, thus reducing the adsorption of the oil phase on the porous medium and lowering the pressure drop. This could enhance the sweep efficiency and hence more oil recovery.



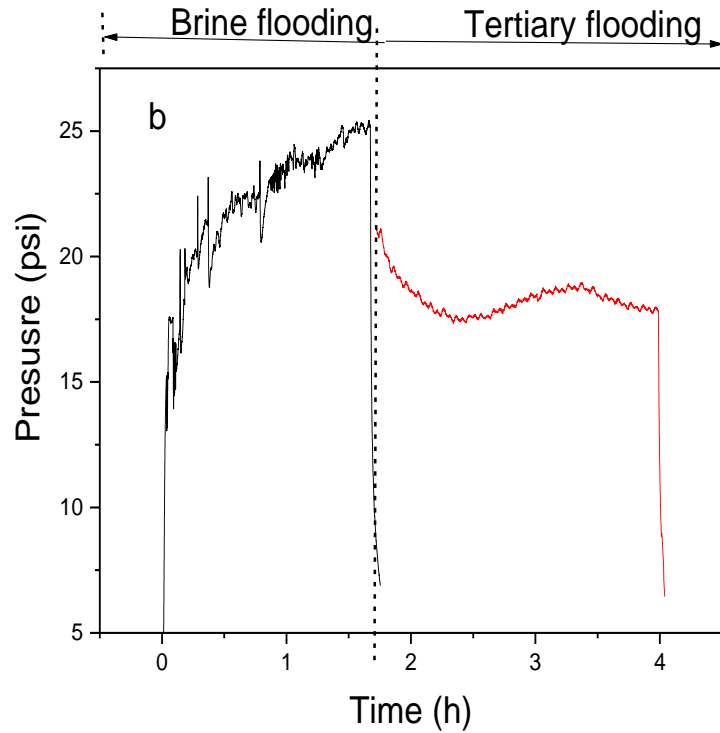


**Figure 10.** The Differential pressure for (a) copolymer containing negative sulfonate group (sample B) and (b) Sample B/MWCNT at high temperature (85°C) and high brine salinity (8 wt. %, NaCl, 2 wt. % CaCl<sub>2</sub> and 2 wt. % MgCl<sub>2</sub>)

Three major mechanisms of oil recovery enhancement (IFT, CA and viscosity) were all investigated in this work and the contribution of those factors was evaluated using the desirability model (**Eqn. 2 and 3**) by demonstrating the relationship between the desirability of the related factor and efficiency of the recovered oil to evaluate the factor with the greater influence to the overall EOR efficiency. Both individual ( $d_i$ ) and combined (D) desirability are used to observe the effect of each factor affecting the EOR. Once a good correlation is accomplished the dominant factor could be extended to predict a trend of the potential relation between the factors and recovery efficiency [70]. IFT, CA and viscosity are selected to examine their influence on the oil recovery efficiency. The results of selected factors for samples used in core flooding experiment are shown in **Table 5** and the analysed desirable values are plotted in **Fig. 11**. As can be seen from **Fig. 11**, only viscosity desirability is able to

imply with the relationship. However, the aforementioned trends of the factor to the % recovery efficiency indicate that viscosity is the favourable mechanism playing a dominant role to recover the high viscous oil from the core, while IFT and CA show less significant changes in the relationship. After combining all three desirabilities (D) no clear correlation with the recovery efficiency was observed.

$$d_i = e^{-e^{-x_i}} \dots \dots \dots \text{Eqn. 2}$$

$$D = \left( \prod_{i=1}^n d_i \right)^{1/n} = \sqrt[n]{d_1 d_2 \dots d_n} \dots \dots \dots \text{Eqn. 3}$$

Where, d stands for the individual desirability function ((i) while n stand for the amount of the affecting factors that are designed to affect the indicator.

**Table 5.** Evaluation of affecting factor (IFT, CA and Viscosity) with their individual desirability ( $d_{IFT}$ ,  $d_{\Theta}$  and  $d_{\mu}$ ) and combined desirability (D) for each fluid use in this experiment.

Fluid	EOR Mechanisms		Individual desirability (d)			Desirability (D)	% Oil recovery efficiency
	IFT(mN/m) $\mu$ (mPa·s)	$\Theta(^{\circ})$	$d_{IFT}$	$d_{\Theta}$	$d_{\mu}$		
Sample A (API)	34.27 3.01	40.18	$2.89 \times 10^{-1}$ $\times 10^{-2}$	$4.10 \times 10^{-1}$	1.29	$1.15 \times 10^{-1}$	7.6
Sample B (API)	34.15 6.88	40.87	$2.84 \times 10^{-1}$ $\times 10^{-1}$	$3.94 \times 10^{-1}$	2.08	$2.85 \times 10^{-1}$	10.6
Sample B + MWCNTs (API)	28.18 16.14	36.86	$7.01 \times 10^{-2}$ $\times 10^{-1}$	$4.84 \times 10^{-1}$	8.71	$3.09 \times 10^{-1}$	14.8
Sample A (pH =11)	55.48 3.55	41.97	$9.16 \times 10^{-1}$ $\times 10^{-2}$	$3.69 \times 10^{-1}$	2.28	$1.97 \times 10^{-1}$	7.0
Sample D (pH =11)	52.11 8.71	42.09	$8.75 \times 10^{-1}$ $\times 10^{-2}$	$3.66 \times 10^{-1}$	4.01	$2.34 \times 10^{-1}$	8.71
Sample D + WMCNTs (pH =11)	47.28 12.59	36.99	$7.83 \times 10^{-1}$ $\times 10^{-1}$	$4.83 \times 10^{-1}$	7.05	$6.43 \times 10^{-1}$	10.8

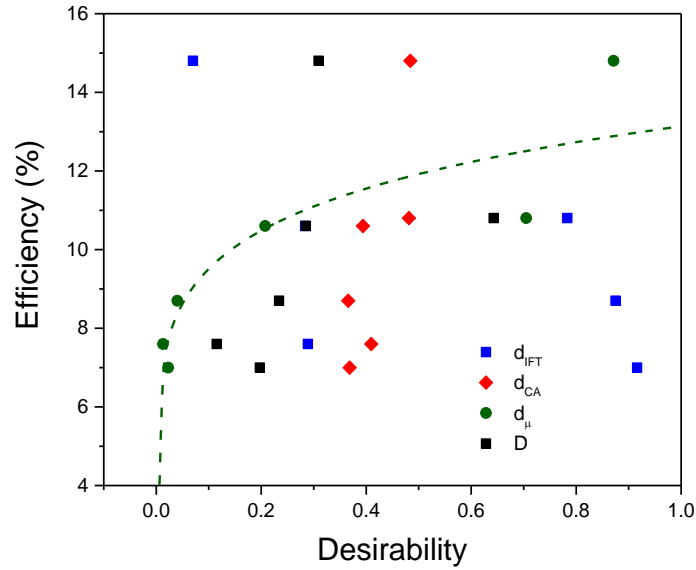


**Figure 11.** % EOR efficiency as a function of overall desirability (D) and individual desirability (d) factors for three EOR mechanism.

#### 4. Conclusion

After secondary EOR, a considerable amount of oil remains trapped in reservoirs and can no longer be recovered using conventional methods. Polymer flooding has been successfully implemented to improved oil recovery in many depleted oil reservoirs. However, the stability of the polymers under harsh conditions is a major challenge for many applications including enhanced oil recovery. This work proposed two new ways to address this issue, by engineering new polymers with improved temperature tolerance and the use of carbon nanotubes. Different modified acrylamide co/ter-polymers were produced from free-radical polymerization and multi walled carbon nanotubes were further introduced to improve the stability of the polymer under high temperature and high salt conditions. The interaction of nanoparticles with the polymer was also characterised. Enhanced oil recovery experiments were also performed and showed the validation of the approach. The following outcomes can be summarised based on the obtained results:

- The polydispersity of different co/ter-polymers was varied by changing various monomers during the polymerization process.
- Addition of MWCNTs improved the viscosity and viscoelasticity of the polymer dispersions.
- The polyampholytic ter-polymer and polyelectrolyte copolymer containing negative sulfonate groups showed better enhancement in both stability and viscosity of MWCNTs/polymer dispersions in alkali and API brine solution respectively.
- Comparing to pure polymer solution, addition of MWCNTs improved the oil recovery efficiency at high temperature (85 °C) in the presence of both alkaline pH and API brine conditions, yet with a lower pressure drop, showing great promise for future EOR applications.
- Despite the fact that the polymer/ MWCNTs have lower interfacial tension and contact angle compared to pure polymer in both alkaline and API brine conditions; the results of desirability function indicated that viscosity is the main factor responsible for high oil recovery.

**Acknowledgement:** This work was funded by European Research Council Consolidated Grant (ERC-2014-CoG, Grant number: 648375) and Petroleum Technology Development Funds (PTDF) Merit PhD Scholarship, Nigeria.

## 5. References

1. Samanta, A., et al., Mobility control and enhanced oil recovery using partially hydrolysed polyacrylamide (PHPA). *International Journal of Oil, Gas and Coal Technology*, 2013. **6**(3): p. 245-258.
2. Tangparitkul, S., et al., Interfacial and Colloidal Forces Governing Oil Droplet Displacement: Implications for Enhanced Oil Recovery. *Colloids and Interfaces*, 2018. **2**(3): p. 30.
3. Pogaku, R., et al., Polymer flooding and its combinations with other chemical injection methods in enhanced oil recovery. *Polymer Bulletin*: p. 1-22.
4. Yang-Chuan, K., W. Guang-Yao, and W. Yi, Preparation, morphology and properties of nanocomposites of polyacrylamide copolymers with monodisperse silica. *European Polymer Journal*, 2008. **44**(8): p. 2448-2457.
5. Deng, S., et al., Produced water from polymer flooding process in crude oil extraction: characterization and treatment by a novel crossflow oil–water separator. *Separation and Purification Technology*, 2002. **29**(3): p. 207-216.
6. Hu, Z., et al., Rheological Properties of Partially Hydrolyzed Polyacrylamide Seeded by Nanoparticles. *Industrial & Engineering Chemistry Research*, 2017. **56**(12): p. 3456-3463.
7. Gao, C., Viscosity of partially hydrolyzed polyacrylamide under shearing and heat. *Journal of Petroleum Exploration and Production Technology*, 2013. **3**(3): p. 203-206.
8. Abidin, A., T. Puspasari, and W. Nugroho, Polymers for enhanced oil recovery technology. *Procedia Chemistry*, 2012. **4**: p. 11-16.
9. Lee, L., J. Lecourtier, and G. Chauveteau, Influence of calcium on adsorption properties of enhanced oil recovery polymers. 1989, ACS Publications.
10. Al-Sabagh, A., et al., Solution properties of hydrophobically modified polyacrylamides and their potential use for polymer flooding application. *Egyptian Journal of Petroleum*, 2016. **25**(4): p. 433-444.
11. Wever, D., F. Picchioni, and A. Broekhuis, Polymers for enhanced oil recovery: a paradigm for structure–property relationship in aqueous solution. *Progress in Polymer Science*, 2011. **36**(11): p. 1558-1628.
12. Maghzi, A., et al., The impact of silica nanoparticles on the performance of polymer solution in presence of salts in polymer flooding for heavy oil recovery. *Fuel*, 2014. **123**: p. 123-132.
13. Zhou, W., et al. Application of hydrophobically associating water-soluble polymer for polymer flooding in China offshore heavy oilfield. in *International Petroleum Technology Conference*. 2007. International Petroleum Technology Conference.
14. Afolabi, R.O., Effect of surfactant and hydrophobe content on the rheology of poly (acrylamide-co-N-dodecylacrylamide) for potential enhanced oil recovery application. *American Journal of Polymer Science*, 2015. **5**(2): p. 41-46.
15. Thomas, A., N. Gaillard, and C. Favero, Some key features to consider when studying acrylamide-based polymers for chemical enhanced oil recovery. *Oil & Gas Science and Technology–Revue d'IFP Energies nouvelles*, 2012. **67**(6): p. 887-902.
16. Zou, C., et al.,  $\beta$ -Cyclodextrin modified anionic and cationic acrylamide polymers for enhancing oil recovery. *Carbohydrate polymers*, 2012. **87**(1): p. 607-613.
17. Chen, Q., et al., Thermoviscosifying polymer used for enhanced oil recovery: rheological behaviors and core flooding test. *Polymer bulletin*, 2013. **70**(2): p. 391-401.

18. Cao, J., et al., Application of Amino-functionalized Nano-silica in Improving the Thermal Stability of Acrylamide Based Polymer for Enhanced Oil Recovery. *Energy & Fuels*, 2017.
19. Roustaei, A., S. Saffarzadeh, and M. Mohammadi, An evaluation of modified silica nanoparticles' efficiency in enhancing oil recovery of light and intermediate oil reservoirs. *Egyptian Journal of Petroleum*, 2013. **22**(3): p. 427-433.
20. Deng, Y., et al., Bonding between polyacrylamide and smectite. *Colloids and Surfaces A: Physicochemical and Engineering Aspects*, 2006. **281**(1-3): p. 82-91.
21. Karimi, A., et al., Wettability alteration in carbonates using zirconium oxide nanofluids: EOR implications. *Energy & Fuels*, 2012. **26**(2): p. 1028-1036.
22. El-Diasty, A.I. and A.M. Aly. Understanding the mechanism of nanoparticles applications in enhanced oil recovery. in *SPE North Africa Technical Conference and Exhibition*. 2015. Society of Petroleum Engineers.
23. Miranda, C.R., L.S.d. Lara, and B.C. Tonetto. Stability and mobility of functionalized silica nanoparticles for enhanced oil recovery applications. in *SPE International Oilfield Nanotechnology Conference and Exhibition*. 2012. Society of Petroleum Engineers.
24. Nourafkan, E., et al., Synthesis of stable nanoparticles at harsh environment using the synergistic effect of surfactants blend. *Journal of Industrial and Engineering Chemistry*, 2018.
25. Nourafkan, E., Z. Hu, and D. Wen, Nanoparticle-enabled delivery of surfactants in porous media. *Journal of colloid and interface science*, 2018. **519**: p. 44-57.
26. Nourafkan, E., Z. Hu, and D. Wen, Controlled delivery and release of surfactant for enhanced oil recovery by nanodroplets. *Fuel*, 2018. **218**: p. 396-405.
27. Hu, Z., et al., Microemulsions stabilized by in-situ synthesized nanoparticles for enhanced oil recovery. *Fuel*, 2017. **210**: p. 272-281.
28. Zhu, D., et al., Aqueous hybrids of silica nanoparticles and hydrophobically associating hydrolyzed polyacrylamide used for EOR in high-temperature and high-salinity reservoirs. *Energies*, 2014. **7**(6): p. 3858-3871.
29. Portehault, D., et al., Hybrid thickeners in aqueous media. *Colloids and Surfaces A: Physicochemical and Engineering Aspects*, 2006. **278**(1-3): p. 26-32.
30. Petit, L., et al., Responsive hybrid self-assemblies in aqueous media. *Langmuir*, 2007. **23**(1): p. 147-158.
31. Okay, O. and W. Oppermann, *Polyacrylamide– Clay Nanocomposite Hydrogels: Rheological and Light Scattering Characterization*. *Macromolecules*, 2007. **40**(9): p. 3378-3387.
32. Giraldo, L.J., et al., The effects of SiO<sub>2</sub> nanoparticles on the thermal stability and rheological behavior of hydrolyzed polyacrylamide based polymeric solutions. *Journal of Petroleum Science and Engineering*, 2017. **159**: p. 841-852.
33. Nourafkan, E., et al., Synthesis of stable iron oxide nanoparticle dispersions in high ionic media. *Journal of Industrial and Engineering Chemistry*, 2017. **50**: p. 57-71.
34. Fu, P., et al., Preparation, stability and rheology of polyacrylamide/pristine layered double hydroxide nanocomposites. *Journal of Materials Chemistry*, 2010. **20**(19): p. 3869-3876.
35. Hu, Z. and G. Chen, Novel nanocomposite hydrogels consisting of layered double hydroxide with ultrahigh tensibility and hierarchical porous structure at low inorganic content. *Advanced Materials*, 2014. **26**(34): p. 5950-5956.
36. Tjong, S.C., Structural and mechanical properties of polymer nanocomposites. *Materials Science and Engineering: R: Reports*, 2006. **53**(3): p. 73-197.

37. Bhardwaj, P., et al., Nanosize polyacrylamide/SiO<sub>2</sub> composites by inverse microemulsion polymerization. *International Journal of Polymeric Materials*, 2008. **57**(4): p. 404-416.
38. Wei, C., Radius and chirality dependent conformation of polymer molecule at nanotube interface. *Nano letters*, 2006. **6**(8): p. 1627-1631.
39. Liu, W., et al., Interactions between single-walled carbon nanotubes and polyethylene/polypropylene/polystyrene/poly (phenylacetylene)/poly (p-phenylenevinylene) considering repeat unit arrangements and conformations: a molecular dynamics simulation study. *The Journal of Physical Chemistry C*, 2008. **112**(6): p. 1803-1811.
40. Yang, M., V. Koutsos, and M. Zaiser, Interactions between polymers and carbon nanotubes: a molecular dynamics study. *The Journal of Physical Chemistry B*, 2005. **109**(20): p. 10009-10014.
41. Mahdavian, A.R., M. Abdollahi, and H.R. Bijanzadeh, Kinetic study of radical polymerization. III. Solution polymerization of acrylamide by <sup>1</sup>H-NMR. *Journal of applied polymer science*, 2004. **93**(5): p. 2007-2013.
42. Durmaz, S. and O. Okay, Acrylamide/2-acrylamido-2-methylpropane sulfonic acid sodium salt-based hydrogels: synthesis and characterization. *Polymer*, 2000. **41**(10): p. 3693-3704.
43. Rosa, F., J. Bordado, and M. Casquilho, Hydrosoluble copolymers of acrylamide-(2-acrylamido-2-methylpropanesulfonic acid). Synthesis and characterization by spectroscopy and viscometry. *Journal of applied polymer science*, 2003. **87**(2): p. 192-198.
44. Liao, Y., et al., UV-initiated polymerization of hydrophobically associating cationic polyacrylamide modified by a surface-active monomer: a comparative study of synthesis, characterization, and sludge dewatering performance. *Industrial & Engineering Chemistry Research*, 2014. **53**(27): p. 11193-11203.
45. Li, X., et al., Optimized preparation of micro-block CPAM by response surface methodology and evaluation of dewatering performance. *RSC Advances*, 2017. **7**(1): p. 208-217.
46. Ranka, M., P. Brown, and T.A. Hatton, Responsive stabilization of nanoparticles for extreme salinity and high-temperature reservoir applications. *ACS applied materials & interfaces*, 2015. **7**(35): p. 19651-19658.
47. Fujigaya, T. and N. Nakashima, Non-covalent polymer wrapping of carbon nanotubes and the role of wrapped polymers as functional dispersants. *Science and technology of advanced materials*, 2015. **16**(2): p. 024802.
48. Nativ-Roth, E., et al., Physical adsorption of block copolymers to SWNT and MWNT: a nonwrapping mechanism. *Macromolecules*, 2007. **40**(10): p. 3676-3685.
49. Ansari, R., S. Ajori, and S. Rouhi, Structural and elastic properties and stability characteristics of oxygenated carbon nanotubes under physical adsorption of polymers. *Applied Surface Science*, 2015. **332**: p. 640-647.
50. Seright, R.S., et al., Stability of partially hydrolyzed polyacrylamides at elevated temperatures in the absence of divalent cations. *Spe Journal*, 2010. **15**(02): p. 341-348.
51. Bagaria, H.G., et al., Iron oxide nanoparticles grafted with sulfonated copolymers are stable in concentrated brine at elevated temperatures and weakly adsorb on silica. *ACS applied materials & interfaces*, 2013. **5**(8): p. 3329-3339.
52. Bagaria, H.G., et al., Stabilization of iron oxide nanoparticles in high sodium and calcium brine at high temperatures with adsorbed sulfonated copolymers. *Langmuir*, 2013. **29**(10): p. 3195-3206.

53. McCormick, C.L. and D. Elliott, Water-soluble copolymers. 14. Potentiometric and turbidimetric studies of water-soluble copolymers of acrylamide: comparison of carboxylated and sulfonated copolymers. *Macromolecules*, 1986. **19**(3): p. 542-547.
54. Albonico, P. and T.P. Lockhart, pH effects on the solubility of polyacrylamides in hard brines. *Journal of applied polymer science*, 1995. **55**(1): p. 69-73.
55. Muller, G., J. Fenyó, and E. Selegny, High molecular weight hydrolyzed polyacrylamides. III. Effect of temperature on chemical stability. *Journal of Applied Polymer Science*, 1980. **25**(4): p. 627-633.
56. Sahoo, N.G., et al., Polymer nanocomposites based on functionalized carbon nanotubes. *Progress in polymer science*, 2010. **35**(7): p. 837-867.
57. Bilalis, P., et al., Non-covalent functionalization of carbon nanotubes with polymers. *Rsc Advances*, 2014. **4**(6): p. 2911-2934.
58. Pramanik, C., et al., Carbon Nanotube Dispersion in Solvents and Polymer Solutions: Mechanisms, Assembly, and Preferences. *ACS nano*, 2017. **11**(12): p. 12805-12816.
59. Noguchi, Y., et al., Single-walled carbon nanotubes/DNA hybrids in water are highly stable. *Chemical Physics Letters*, 2008. **455**(4-6): p. 249-251.
60. Hussein, I.A., et al., Rheological behavior of associating ionic polymers based on diallylammonium salts containing single-, twin-, and triple-tailed hydrophobes. *European Polymer Journal*, 2010. **46**(5): p. 1063-1073.
61. Yasuda, K., K. Okajima, and K. Kamide, Study on Alkaline Hydrolysis of Polyacrylamide by <sup>13</sup>C NMR. *Polymer journal*, 1988. **20**(12): p. 1101.
62. Ma, Q., et al., Theoretical studies of hydrolysis and stability of polyacrylamide polymers. *Polymer Degradation and Stability*, 2015. **121**: p. 69-77.
63. Hirasaki, G.J., C.A. Miller, and M. Puerto. Recent advances in surfactant EOR. in *SPE Annual Technical Conference and Exhibition*. 2008. Society of Petroleum Engineers.
64. Pötschke, P., et al., Rheological and dielectrical characterization of melt mixed polycarbonate-multiwalled carbon nanotube composites. *Polymer*, 2004. **45**(26): p. 8863-8870.
65. Cassagnau, P., Linear viscoelasticity and dynamics of suspensions and molten polymers filled with nanoparticles of different aspect ratios. *Polymer*, 2013. **54**(18): p. 4762-4775.
66. Kedar, V. and S.S. Bhagwat, Effect of salinity on the IFT between aqueous surfactant solution and crude oil. *Petroleum Science and Technology*, 2018. **36**(12): p. 835-842.
67. Bera, A., A. Mandal, and B. Guha, Synergistic effect of surfactant and salt mixture on interfacial tension reduction between crude oil and water in enhanced oil recovery. *Journal of Chemical & Engineering Data*, 2013. **59**(1): p. 89-96.
68. Nikolov, A., K. Kondiparty, and D. Wasan, Nanoparticle self-structuring in a nanofluid film spreading on a solid surface. *Langmuir*, 2010. **26**(11): p. 7665-7670.
69. Wasan, D.T. and A.D. Nikolov, Spreading of nanofluids on solids. *Nature*, 2003. **423**(6936): p. 156.
70. Tangparitkul, S., Evaluation of effecting factors on oil recovery using the desirability function. *Journal of Petroleum Exploration and Production Technology*, 2018: p. 1-10.